

Some Phenomenological and Basic Models in Fuel Rod Simulation

S. Harriague, E.J. Savino, C.A. Baigorria

N.S. de De Grande

Departamento de Materiales, Comision Nacional de Energia Atomica, Av. del Libertador 8250, 1429 Buenos Aires, Argentina

Summary

In this paper we couple some basic, physically sound models of material and rod ensemble behaviour to the BACO code. This code describes the overall fuel performance within a stable, consistent and modularly structured thermomechanical system.

The effect of pellet cracking and relocation on the fuel temperature distribution is considered within a phenomenological model which includes pellet relocation via circumferential cracks. Cases B and C of EPRI benchmarking are simulated and experimental result, satisfactorily reproduced.

A Zry irradiation growth and creep model based on rate theory is coupled to BACO. The influence of different vacancy migration and formation energies reported in the literature is studied.

1. Introduction

Fuel simulation codes are generally highly complex computer systems aiming to predict the fuel rod thermomechanical performance. A large number of them are based on a set of empirical material or ensemble behaviour laws fitted "ad hoc" for reproducing the rod behaviour at a particular reactor and for a given fuel or experiment design. But if the laws adopted are of narrow validity, when the reactor condition or the fuel design are even slightly changed the agreement between predictions and experiments may be lost.

Our approach to fuel simulation is then based on only using models that, although fitted to a limited number of experimental points, are based on physically sound theories of general validity ⁽¹⁾. It is felt this approach should provide at least qualitative agreement with a large variety of fuel designs and irradiation conditions. In addition, within our approach, a poor agreement shows that the material models or parameters used are inappropriate under the numerical experiment boundary conditions. They can then be improved and our knowledge of the laws governing material or ensemble behaviour may be increased by this procedure. Within this spirit, two examples of the way we test materials and rod ensemble laws for our fuel simulation code BACO ⁽²⁾ are presented in this paper.

In case C of the EPRI report ⁽³⁾ on fuel code benchmarking, all codes predict a central fuel temperature larger than the experimental one. This fact agrees with the Broughton and Mac Donald (BMD) ⁽⁴⁾ observation that the fuel temperature calculated with large hot gaps gives poor agreement with experiments when the Ross and Stoute ⁽⁵⁾ or similar models are used for gap conductance. The case C of EPRI is then used for testing whether including a model of partial gap closing by pellet relocation proposed by BMD provides a better agreement between predictions and experiments. The same EPRI report provides a way of completing the test. For another set of fuel irradiations, case B, most of the codes give a reasonable temperature prediction. For consistency any fitting of the gap conductance which improves the prediction of case C must not spoil that agreement in case B.

In the second part of the paper the Zry cladding mechanical behaviour is simulated by a rate theory model of growth and creep coupled with thermoelasticity based on the work of Savino and Laciana ⁽⁶⁾ (SL). This calculation proves the feasibility of self consistently adapting basic, general models of material behaviour into complex, multi-parametric thermomechanical algorithms. The easiness in adapting different models into BACO proves once more the advantage of possessing a code based in a self-consistent, quickly convergent and stable numerical method being, at the same time, modularly structured.

2. Pellet-Cladding heat transfer

When a nominal hot gap is predicted by a mechanical calculation, BMD ⁽⁴⁾ proposed its effective fuel to cladding thermal conductance to be

$$h_{\text{gap}} = (1 - F) h_o + F h_c \quad (1)$$

where h_o is the nominal conductance of the open gap and h_c the one of a closed one at zero contact pressure; while F is the pellet fraction in contact with the cladding. This fraction was adjusted to experiments via an inverse power law of the hot radial gap (Δr)

and radius of the pellet (R_p):

$$F = \frac{1}{a_1 \left(\frac{\Delta r}{R_p} \right)^{a_2} + 1.429} + 0.3 \quad (2)$$

(2) depends on the empirical constants a_1 and a_2 , which are themselves functions of the burnup. The same values reported by BMD for (1) and (2) are used in this work. However, an improvement is proposed within that same model. Though (as noted by Maki and Meyer⁽⁷⁾) fuel relocation necessarily implies a change in pellet conductance, this is not included by BMD. They assume relocation to occur by radial cracks in the pellet which should not greatly affect its conductivity. However, due to the large creep at the central region, a fraction of circumferential cracking within the pellet is necessary for relocation. This is assumed by us to occur by circumferential cracking of the pellet at given radii $r = r_1, \dots, r_n$ (n usually 1 or 2). Those cracks join to the surface by radial ones. A discontinuous temperature distribution is assumed inside the pellet with jumps at the radius r_j :

$$\Delta T (r_j) = \frac{q (r_j)}{2\pi r_j h_j} \quad (3)$$

where q is the heat flux at r_j and

$$h_j = (1 - F) h_c (r_j) + F h_o (r_j) \quad (4)$$

where the closed (h_c) and open (h_o) conductance of an inner gap within the UO_2 pellet are calculated at the corresponding local temperature and h_c at contact pressure $p_c = -\sigma_r$ at r_j , while h_o for an inner gap width $\Delta r_j = \Delta r/n$, where Δr : pellet-cladding gap width.

In Fig. 1 the EPRI benchmarking temperatures for case C are plotted against burnup. It can be seen that the 5 codes tested overpredict the central temperature. In Fig. 2 we show our results with BACO when different gap conductance models are used. It can be seen that the parametric adjust of Lassmann⁽⁸⁾ to a large number of experiments also overpredicts the fuel central temperature. On the contrary, by using either the simple BMD model or its modified version by including one inner crack, the temperature is slightly underpredicted, while if two circumferential cracks are included the fitting between experiments and theory is remarkably good. In figures 3 and 4 the temperatures predicted by BACO in case B of EPRI for the carriages MZL and MZK are plotted together with the corresponding power cycle. The BMD model modified with the indicated number of circumferential cracks is used. It can be seen the agreement between experiments and predictions is retained in this case.

3. Cladding thermomechanical behaviour

We plot in Fig. 5 the results of Zry tubes creep under irradiation reported by Frenkel and Weisz⁽⁹⁾ as a function of the irradiation time. They correspond to three different final annealing temperatures of the tubes. Also the results for Zry creep as predicted by different laws reported in the literature are plotted in the same figure^(3,10-14). It

can be seen that not only a large dispersion exists among different predictions and that they do not fit the experimental data, but also that relevant parameters as tube texture or stress relieving are not included in the models, while they affect the experiment.

SL⁽⁶⁾ proposed to calculate within a unique model the total deformation and intergranular stresses due to prismatic edge dislocation climbing in hcp lattice by preferential attraction of interstitials as compared to vacancies, irradiation growth and stress induced preferential attraction (SIPA)⁽¹⁵⁾ of interstitials for dislocations favourably oriented with respect to intergranular stresses⁽¹⁶⁾. The texture is simulated by a discrete of grain orientations, and the Taylor hypothesis of equal strain for all orientations is imposed. In this paper we assume the total strain rate for each grain to be composed of a contribution due to dislocation climb by growth, SIPA and thermal vacancy emission and vacancy absorption at grain boundaries, plus anisotropic thermal expansion and elastic strain rates which compensate among themselves in order to satisfy Taylor hypothesis. A more detailed paper describing the model will be published soon⁽¹⁷⁾.

The cladding is divided into a discrete number of radial sections and within each one the above described model is represented by a set of equations. The section average stress and strain can be formally written as a function of the intergranular stresses being solution of those equations. These average stresses and the strains must also satisfy the boundary conditions for the cladding as well as the continuity and equilibrium equations⁽²⁾. All this constitutes a system of equations for the average stresses at each section, the stresses at each orientation and at each section, and the strain increments at each section. The system is solved by implicit finite differences over the irradiation history, and coupled with the whole system of equations in BACO⁽²⁾ for the pellet thermomechanical behaviour, rod thermal behaviour and fission gas release.

With the purpose of showing some representative results, a simple cycle consisting of a 12h. power up ramp from 0 to 300 W/cm and a stay of 100 days at constant power is simulated for a natural uranium, Zry cladded cylindrical rod under a fast neutron flux of 7×10^{13} n/cm²s. The cladding texture is represented by three grain orientations at each section, with the c axis on an axial cladding plane and at: 1 - 0°; 2 - ± 30°; 3 - ± 55° from the cladding radial direction, the respective densities being N(1) = 0.12; N(2) = 0.36; N(3) = 0.52. This way of modelling the cladding is extremely sensitive to the microstructural parameters, such as texture, grain size, dislocation density, etc.

For the case of Zr and its alloys there is a long dated controversy on the values of the vacancy diffusion and formation energy in the α phase. On one side Hood sustains this metal is normal⁽¹⁸⁾ while Dymant et al.⁽¹⁹⁾ claim an anomalous effect. In a paper by Pedraza et al.⁽²⁰⁾, where our growth model was first reported, the values for vacancy migration energy $E_m^v = 1.2$ eV, diffusivity constant $D_{ov} = 0.38$ cm²s⁻¹ and formation energy $E_v^v = 1.2$ eV, consistent with Dollins⁽²¹⁾ and Hood⁽¹⁸⁾, were adopted. A set consistent with Dymant et al. results⁽¹⁹⁾ is $E_m^v = 0.67$ eV; $D_{ov} = 0.11 \times 10^{-7}$ cm²s⁻¹; $E_f^v = 0.67$ eV⁽²²⁾. While in the first case only irradiation is effective as a defects source for inducing the dislocation climb at reactor conditions, in the second irradiation plus thermal creep by vacancy emission may be relevant at reactor temperature. For both sets of data, representative strain rates and stresses are plotted in Figs. 6/9. There, for the inner cladding radius, the calculated strain rate components are plotted in Figs. 6 and 7 by

using the two sets of vacancy diffusivity and formation values above reported. Both, the total strain rates in the main axes directions, and the strain rates due to dislocation climb and grain boundary shrinkage (permanent strain) for the grain orientation with the largest volume density (orientation 3) are plotted as a function of irradiation time. In Figs. 8 and 9 the calculated average stresses are plotted together with the intergranular stresses over orientation 3; care must be taken in looking at these results that are reported respectively in the specimen and grain axes. The complete analysis of these curves exceeds the length and purpose of this paper, there are however some facts which can be consistently discussed. For example due to the texture, the strain rate independent of the stress in the axial direction (axial growth) must be positive. Then in the case of high migration and formation energy for the vacancy, where the predominant effect is stress independent growth, the axial strain rate is positive (Fig. 6). On the contrary, when the stress and vacancy thermal emission are important, the axial creep dominates and this is negative (the same sign of the average σ_A in Figs. 8 and 10). We see that in the case of relatively small formation and migration energy (Dyment et al. data), the axial strain rate becomes negative (Fig. 7). For both cases the axial strain rate increases as a function of the irradiation time due to the calculated reduction of the intergranular stress σ_b^3 over grain orientation 3 in the direction b normal to the tube axis A, which is parallel to a over the basal plane. The fact that only basal Burgers vectors of the dislocations are included in the model necessarily implies a difference on tangential creep strain (ϵ_T) for internal and external pressure. For external pressure in a closed end tube, that is the case studied, we find that, when creep dominates, the tangential strain rate ($\dot{\epsilon}_T$) is positive, as in Fig. 7.

4. Summary and conclusions

In this paper the need of using physically sound models of material and ensemble behaviour for fuel rod simulation is consistently expressed. It is founded by means of two examples.

In one it is shown that allowing for pellet relocation in the pellet-clad gap provides gap heat conductance expressions which fit better to experiments than the usual laws based on Ross-Stoute work ⁽⁵⁾. The perfect agreement obtained in the cases studied must however be taken with care. The gap conductance parameters are taken from BMD work ⁽⁴⁾; this does not include a full pellet relocation model as proposed by us above. Then, although we found those values as sensible, a proper fit to experiment should be done for obtaining the best available model of gap conductance within our modified version of BMD.

In a second example a basic theory of dislocation climb is used for describing the Zry cladding thermomechanics. This approach is rather promising. In this paper we have proved the feasibility of coupling a complex mechanical simulation code like BACO with basic material models. We postpone for a forecoming paper ⁽¹⁷⁾ a deeper study of the results advanced in Section 3.

Acknowledgement

We acknowledge partial support from the "Proyecto Multinacional de Tecnología de Materiales" OEA-CNEA.

References

- (1) HARRIAGUE, S., SAVINO, E.J., COROLI, G., BASOMBRI, F.G. and SANCHEZ SARMIENTO, G., "Theoretical Fuel Modelling at CNEA", Nucl. Eng. Design 56, 83-89 (1980).
- (2) HARRIAGUE, S., COROLI, G. and SAVINO, E.J., "BACO (Barra Combustible), a Computer Code for Simulating a Reactor Fuel Rod Performance", Nucl. Eng. Design 56, 91-103 (1980).
- (3) FREEBURN, M.R., PATI, S.R., FIERO, I.B. and ANDREWS, M.G., "Light Water Reactor Fuel Rod Modeling Fuel Code Evaluation", EPRI NP 369 (1977).
- (4) BROUGHTON, J.M. and MAC DONALD, P.E., "Gap Heat Transfer" in "MATPRO-Version 09", TREE-NUREG 1005 (1976).
- (5) ROSS, A.M. and STOUTE, R.L., AECL 1552 (1962).
- (6) SAVINO, E.J. and LACIANA, C.E., "Radiation Induced Creep and Growth of Zirconium Alloys", J. Nucl. Mat. 90, 89-107 (1980).
- (7) MAKI, J.T. and MEYER, J.E., "LWR Fuel Performance Analysis. Fuel Cracking and Relocation", Tech. Rep. MIT-EL 78-038 (1978).
- (8) LASSMANN, K., "Zum Wärmedurchgang in Bereich zwischen Hülle und Brennstoff eines Brennstabes", Wärme und Stoffübertragung 12, 185-202 (1979).
- (9) FRENKEL, J.M. and WEISZ, M., "Effect of the Annealing Temperature on the Creep Strength of Cold Worked Zircaloy-4 Cladding", Zirconium in Nuclear Applications, ASTM STP 551, American Society for Testing and Materials, 140-144 (1974).
- (10) PANKASKIE, O.J., "An Analytical Computer Code for Calculating Creep Buckling of an Initially Oval Tube", BNWL-1784, Richland, Washington, p. 65 (1974).
- (11) GITTUS, I.H., HOWL, D.A. and HUGHES, H., "Theoretical Analysis of Cladding Stresses and Strains Produced by Expansion of Cracked Fuel Pellets", Nucl. Appl. Technol. 9, 40 (1970).
- (12) "MATPRO - Version 10", TREE-NUREG 1180 (1978).
- (13) ROSS-ROSS, P.A. and HUNT, C.E.L., "The In-Reactor Creep of Cold-Worked Zircaloy-2 and Zirconium-2.5% Niobium Pressure Tubes", J. of Nucl. Mater. 26, 2-17 (1968).
- (14) YUNG LIU, Y., BEMENT, A.L., "A Regression Approach for Zircaloy-2 in Reactor Creep Constitutive Equations", IV SMIRT Conference, San Francisco, California, Paper C 3/3 (1977).
- (15) BULLOUGH, R. and WILLIS, J.R., "The Stress Induced Point Defect Dislocation Interaction and its Relevance to Irradiation Creep", Phil. Mag. 31, 855-862 (1975).
- (16) NICHOLS, F.A., "On the SIPA Contribution to Radiation Creep", J. of Nucl. Mat. 84, 207-221 (1979).
- (17) SMETNIANSKY-DE GRANDE, N., POCHEITINO, A., HARRIAGUE, S. and SAVINO, E.J., to be published.
- (18) HOOD, G.M., "The Vacancy Properties of α -Zr", J. of Nucl. Mat. 96, 372-374 (1981).
- (19) DYMENT, F., LIBANATI, C.M., "Self-Diffusion of Ti, Zr and Hf in their HCP Phases and Diffusion of Nb⁹⁵ in HCP Zr", J. of Materials Science 3, 349-359 (1968).
- (20) FAINSTEIN-PEDRAZA, D., SAVINO, E.J. and PEDRAZA, A.J., "Irradiation Growth of Zirconium Base Alloys - Part I", J. of Nucl. Mat. 73, 151-168 (1978).
- (21) DOLLINS, C.C., "In-Pile Dimensional Changes in Newton Irradiated Zirconium Base Alloys", J. of Nucl. Mat. 59, 61-76 (1976).
- (22) DYMENT, F., Private communication.

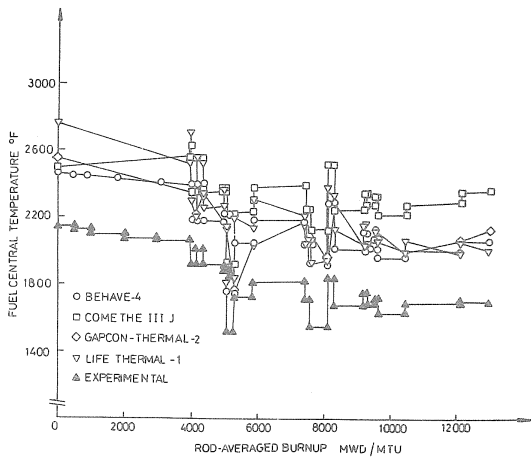


Fig. 1 Predicted and experimental fuel central temperatures against burnup, EPRI's case C (3).

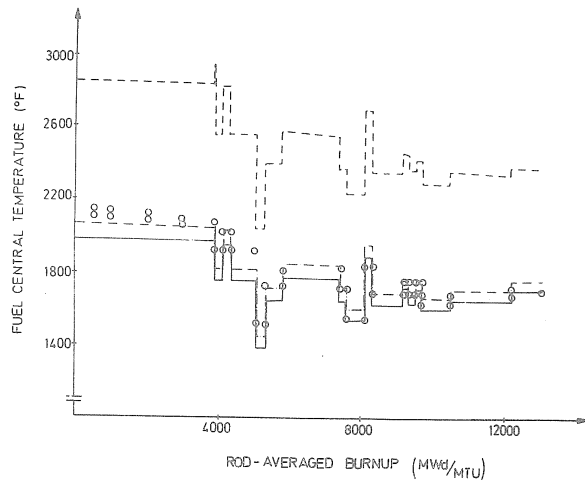


Fig. 2 Measured and calculated fuel central temperature for case C of EPRI's report (3). BACO's predictions: broken line; simulation by using Lessmann's parametric model (8) for fuel-cladding gap heat conductivity. Full line; BMD (4) model, it agrees within drawing precision with the predicted temperature for the modified model with 1 inner circumferential crack at 2/3 of the pellet radius ($r_1 = 2/3 R_p$) to allow for relocation. Broken-dot line; BMD (4) model modified with 2 inner cracks at 1/3 and 2/3 of pellet radius ($r_1 = 1/3 R_p$; $r_2 = 2/3 R_p$). \odot : experimental points.

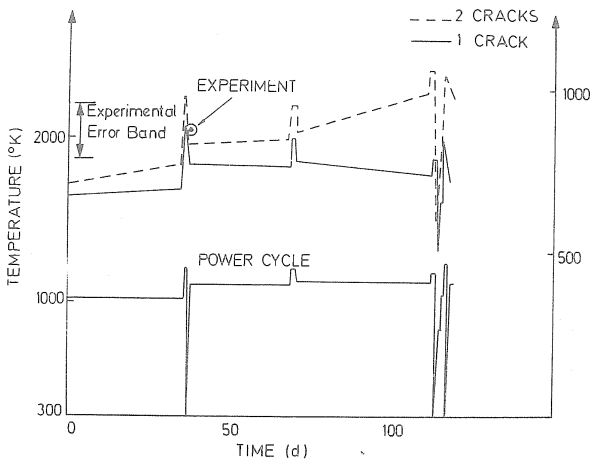


Fig. 3 Power cycle and fuel central temperatures against burnup for carriage MZL of EPRI's case B (3). The modified BMD model (4) is used to calculate the central temperature. Different number of circumferential inner cracks is used for simulating the relocation. Measured values are reported: \odot .

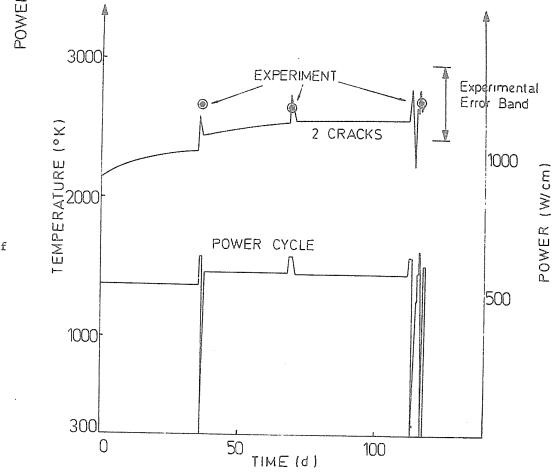


Fig. 4 Power cycle and fuel central temperature are reported as in Fig. 3, for EPRI's case B, carriage MZK (3).

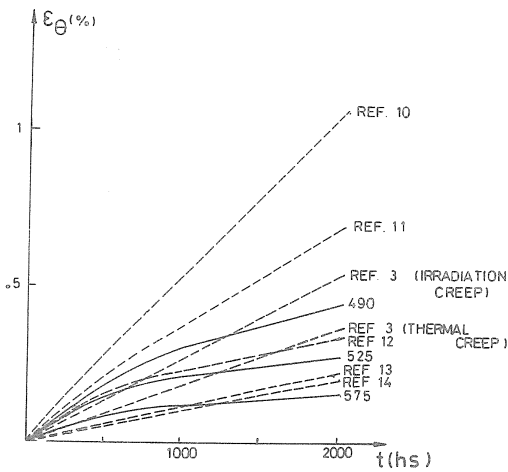


Fig. 5 Irradiation creep of Zry-4 tubes according to Frenkel and Weisz (9). The tangential strain at a temperature of 350°C is reported for a fast neutron flux of 10^{14} n/cm² sec, under a tangential stress of 102 MPa. The tubes have been preannealed for two hours at 490, 525 and 575°C respectively. In dotted line, the creep predicted by different laws in the literature (3, 10-14) is plotted.

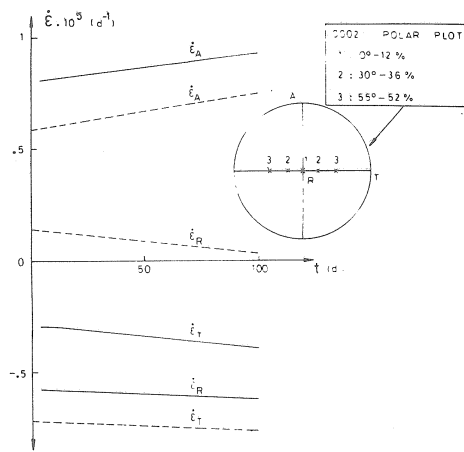


Fig. 6 Calculated cladding strain rate for a cycle of 12 hours power ramp from 0. to 300. W/cm and 100 days at constant power.
 Full line: total strain rate.
 Dotted line: permanent strain rate for orientation 3.
 Vacancy formation and migration parameters: $E_m^V = 1.2$ eV, $D_{OV} = 0.38$ cm² sec⁻¹, $E_F^V = 1.2$ eV.
 The grain orientation densities are also shown at a polar plot. A : axial; T : tangential, R : radial direction.

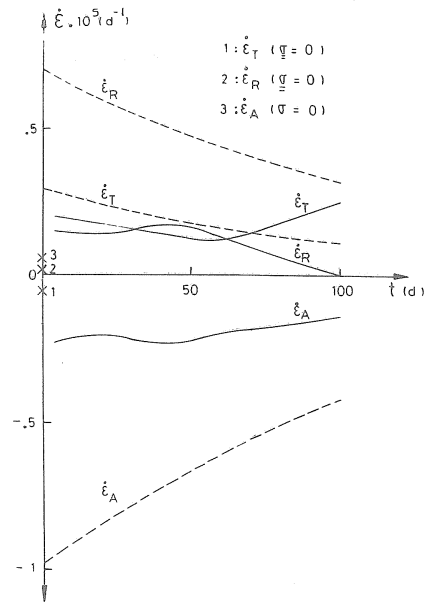


Fig. 7 Calculated cladding strain rates. Idem than in Fig. 6 but for $E_m^V = .67$ eV, $D_{OV} = 1.1 \times 10^{-8}$ cm² sec⁻¹, $E_F^V = .67$ eV.

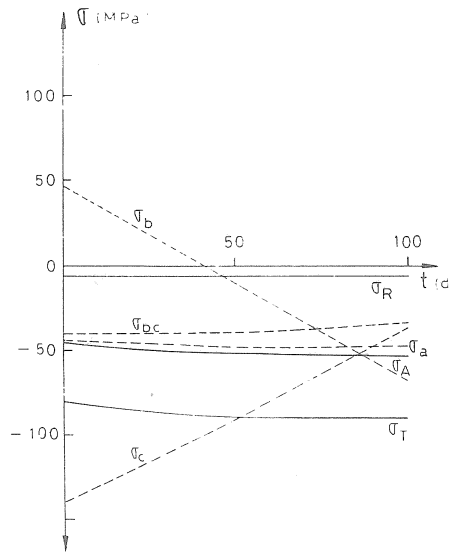


Fig. 8 Calculated stresses corresponding to the strains reported in Fig. 6.
 Full line: average stresses in cladding main axes.
 Dotted line: intergranular stresses on orientation 3; σ_a , σ_b ; stresses over basal plane, σ_c : normal to basal plane. The direction \underline{a} agrees with the axial cladding direction.

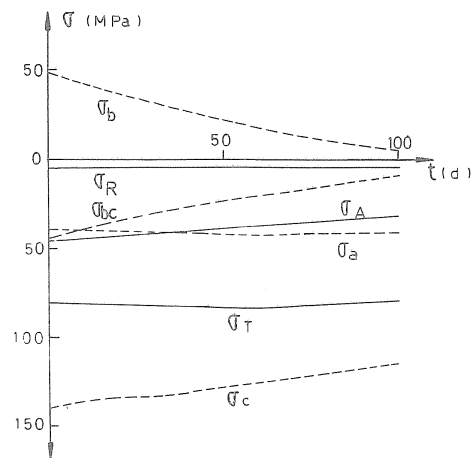


Fig. 9 Calculated stresses corresponding to the strains reported in Fig. 7.